C295/84

Nonlinear unbalance response and stability thresholds of a warped multimass rotor in misaligned bearings

H SPRINGER, Dipl-Ing, Dr Tech and H ECKER, Dipl-Ing
Department of Mechanical Engineering, Technical University of Vienna, Austria
E J GUNTER
Department of Mechanical and Aerospace Engineering, University of Virginia, USA

SYNOPSIS A second order perturbation method is presented to calculate nonlinear unbalance orbits of a multimass rotor supported by misaligned journal bearings. The theory of short journal bearings is employed to determine analytical expressions for first and second order bearing characteristics to be applied in the perturbation approach. It is shown that for many practical applications a good agreement between second order unbalance response and exact numerical solutions is obtained. Both static bearing loads of a multibearing system and stability thresholds of the rotor are calculated in terms of bearing misalignment. Ranges of high sensitivity of the stability thresholds with respect to bearing misalignment can be observed which may explain significant deviations between theoretical predictions and experimental data.

1 INTRODUCTION

Nonlinear bearing characteristics, bearing misalignments, and residual shaft bow are present in almost any real rotor-bearing system and may considerably change its dynamical properties. Since an exact mathematical treatment of the influences of bearing nonlinearities, misalignments, and shaft bow is rather complicated it is desirable to have approximate solution techniques which can easily be applied by design engineers to most of their practical problems.

Nicholas, et al (1) discussed the influence of shaft bow upon the unbalance response of a flexible Jeffcott rotor in two isotropic bearings. Bannister (2) introduced twenty numerically evaluated second order bearing coefficients in order to determine nonlinear unbalance response. Stationary bearing loads of statically indeterminate multibearing systems including nonlinear oil film effects are calculated in (3), and Nasuda (4), investigated the influence of bearing misalignments upon stability limits. Nonlinear unbalance response and stability limits of a rigid Jeffcott rotor in two short journal bearings are obtained in (5) by applying an averaging method.

In this paper Bannister's method (2) of introducing second order bearing coefficients is applied to the theory of short journal bearings and simple analytical expressions for those coefficients are presented. Furthermore, the short bearing characteristics are used to determine the static equilibrium position of a multimass rotor in a misaligned multibearing system. Since simple analytical expressions are available to determine static bearing loads for short journals the numerical effort to calculate stability thresholds is reasonably low even for rather complicated systems. It is shown also that for small values of unbalance and residual shaft bow a nonlinear unbalance response of the rotor may approximately be obtained from a linear recursive routine using first and second order bearing characteristics.

2 THEORY

2.1 Equations of motion

Fig 1 shows the non-assembled configuration of a rotor bearing system. Initial shaft bow and bearing misalignments are defined with respect to the center line (z-axis) between the first and the last bearing station. From this, shaft bow and lateral bearing misalignment for a n-stations model of the rotor may be represented in the form

$$\{\delta(t)\} = \{\delta_1 C_1(t),\ldots,0,\ldots,\delta_j C_j(t),\ldots,0,\ldots,\delta_n C_n(t)\,|\,\delta_1 S_1(t),\ldots,0,\ldots,\delta_j S_j(t),\ldots,0,\ldots,\delta_n S_n(t)\}^T \quad (1)$$

and

$$\{m\} = \{m_{1x},\ldots,0,\ldots,m_{jx},\ldots,0,\ldots,m_{nx}\,|\,m_{1y},\ldots,0,\ldots,m_{jy},\ldots,0,\ldots,m_{ny}\}^T \quad (2)$$

respectively. In Equation (1) $C_j(t) = \cos(\omega t+\beta_j)$ and $S_j(t)=\sin(\omega t+\beta_j)$ with ω being the angular speed of the shaft. At stations where no bearings are located the corresponding misalignment values in Equ.(2) are defined to zero. The influence of slope misalignments between the shaft and the bearing axis is neglected in this investigation, see (2).

The equations of motion of the rotor are described with respect to the x-y-z reference frame as defined in Fig 1

$$[M]\{\ddot{z}\}+([C_E]+[C_I])\{\dot{z}\}+([K_S]+[K_I])\{z\} = \{F_o\}+[K_S]\{\delta(t)\}+\omega^2\{U(t)\}+\{F_B(\{z\}-\{m\},\{\dot{z}\},\omega)\} \quad (3)$$

where

$$\{z\} = \{x_1,\ldots,x_n\,|\,y_1,\ldots,y_n\}^T \quad (4)$$

is the vector of lateral displacements of the shaft at the various stations in x- and y-direction, respectively. $[M]$, $[C_E]$, $[C_I]$ are symmetric matrices which represent mass and external and internal damping characteristics, respectively, of the rotor. Note that gyroscopic effects are not considered in Equ.(3). $[K_S]$ and $[K_I]$ are symmetric and skew-symmetric stiffness matrices due to shaft flexibility and internal damping, respectively. Note that $[K_S]$ and $[K_I]$ are singular. $\{F_o\}$ is a static load vector due to weight, for example, and $\{\delta(t)\}$ is the shaft bow as given in Equ.(1). The unbalance excitation is described by

$$\{U(t)\} = \{M_1 e_1 \cos(\omega t+\Phi_1),\ldots,M_n e_n \cos(\omega t+\Phi_n) \mid M_1 e_1 \sin(\omega t+\Phi_1),\ldots,M_n e_n \sin(\omega t+\Phi_n)\}^T \tag{5}$$

with e_i being the unbalance eccentricities at stations i = 1,2,...n. For the reason of simplicity unbalance couples are not considered here. Nonlinear bearing forces acting upon the rotor are described by a nonlinear vector function $\{F_B(\{x\}, \{\dot{x}\},\omega)\}$which appears at the right hand side of Equ.(3).

2.2 Perturbation approach

In many practical applications as horizontal machines, for example, the unbalance and shaft bow excitation forces are small compared with the static weight forces such that

$$\omega^2\{U(t)\}+[K_S]\{\delta(t)\} \equiv \varepsilon\{F_\omega(t)\} << \{F_o\} \tag{6}$$

holds in Equ.(3) where $\varepsilon<<1$ is a small parameter and $\{F_\omega(t)\}$ is of same order of magnitude as the static load vector $\{F_o\}$.

By expanding the shaft displacements into a series of the form

$$\{z(t)\} = \{z_o\} + \sum_k \{z_k(t)\} = \{z_o\} + \sum_k \varepsilon^k \{\zeta_k(t)\} \tag{7}$$

the nonlinear bearing forces can be expressed up to second order terms as follows

$$\begin{aligned}\{F_B(\{z\}-\{m\},\{\dot{z}\},\omega)\} &= \\ =\{F_B(\{z_o\}-\{m\},\{0\},\omega)\}&- \sum_k \varepsilon^k([K_B]\{\zeta_k\}+[C_B]\{\dot{\zeta}_k\})- \\ - \frac{1}{2}\sum_i \sum_j \varepsilon^{i+j}&(\{\zeta_i\}^T\langle KK_B\rangle\{\zeta_j\}+2\{\zeta_i\}^T\langle KC_B\rangle\{\dot{\zeta}_j\}+ \\ &\{\dot{\zeta}_i\}^T\langle CC_B\rangle\{\dot{\zeta}_j\})\end{aligned} \tag{8}$$

After inserting the above equations into the equations of motion (3) and truncating the expansion by neglecting terms of $O(\varepsilon^3)$ it follows

$$([K_S]+[K_I])\{z_o\} = \{F_o\}+\{F_B(\{z_o\}-\{m\},\{0\},\omega)\} \tag{9}$$

$$[M]\{\ddot{z}_1\}+[C]\{\dot{z}_1\}+[K]\{z_1\} = [K_s]\{\delta(t)\}+\omega^2\{U(t)\} \tag{10}$$

$$[M]\{\ddot{z}_2\}+[C]\{\dot{z}_2\}+[K]\{z_2\} = -\frac{1}{2}\{z_1\}^T\langle KK_B\rangle\{z_1\}- -\{z_1\}^T\langle KC_B\rangle\{\dot{z}_1\}-\frac{1}{2}\{\dot{z}_1\}^T\langle CC_B\rangle\{\dot{z}_1\} \tag{11}$$

where

$$\begin{aligned}[K] &= [K_S] + [K_I] + [K_B] \\ [C] &= [C_E] + [C_I] + [C_B] .\end{aligned} \tag{12}$$

Equ.(9) represents a set of 2n nonlinear relations to be solved for the static equilibrium position $\{z_o\}$ of the shaft for a given misalignment $\{m\}$. From the linear set of differential equations (9) and (10) $\{z_1\}$ and $\{z_2\}$, respectively, can be solved in a recursive manner. The final solution including second order terms is then composed in the form

$$\{z(t)\} = \{z_o\} + \{z_1(t)\} + \{z_2(t)\} + \ldots \tag{13}$$

In Equ.(8) to (12) $[K_B]$ and $[C_B]$ are wellknown bearing stiffness and damping matrices of first order to be calculated at the equilibrium state $\{x_o\} = \{z_o\} - \{m\}$ and $\{\dot{z}\} = \{0\}$. Second order bearing coefficients to be taken at the same equilibrium state are assembled in three-dimensional spatial matrices as

$$\langle KK_B\rangle = -\left[\frac{\partial^2 F_{Bi}}{\partial z_j \partial z_k}\right]\Bigg|_o \tag{14}$$

for stiffness, and

$$\langle KC_B\rangle = -\left[\frac{\partial^2 F_{Bi}}{\partial z_j \partial \dot{z}_k}\right]\Bigg|_o \tag{15}$$

for stiffness-damping, and

$$\langle CC_B\rangle = -\left[\frac{\partial^2 F_{Bi}}{\partial \dot{z}_j \partial \dot{z}_k}\right]\Bigg|_o \tag{16}$$

for damping, where i, j, k = 1,2,...2n indicate the plane, row, and column numbers, respectively, of the above matrices. It can be shown that each plane of $\langle KK_B\rangle$ and $\langle CC_B\rangle$ is symmetric with respect to its rows and columns while $\langle KC_B\rangle$ is not symmetric. Therefore, each bearing of the rotor contributes with twenty independent second order coefficients to the system. In Equ.(8) and (11) symbolic expressions of the form $\{a\}^T\langle KK\rangle\{b\}$ appear. This operation performs a column vector of which the i'th component is the bilinear form of $\{a\}$ and $\{b\}$ with respect to the square matrix located in the i'th plane of the spatial matrix $\langle KK\rangle$. In general, the number of bearings in a real rotor bearing system is much less than the number of stations. Therefore, the spatial matrices $\langle KK_B\rangle$, $\langle KC_B\rangle$, and $\langle CC_B\rangle$ are extremely weak populated and an economic storage scheme is recommended when calculating the right hand side of Equ.(11); see Ref.(6).

2.3 Characteristics of the short journal bearing

In a local r-t-z reference frame of a single bearing, as shown in Fig 1, the bearing characteristics can be evaluated in terms of the static shaft eccentricity ε_o and a corresponding modified Sommerfeld reciprocal

$$S = S_o\left(\frac{L}{D}\right)^2 = \frac{(1-\varepsilon_o^2)^2}{\pi\varepsilon_o\sqrt{16\varepsilon_o^2+\pi^2(1-\varepsilon_o^2)}} \tag{17}$$

where $S_o = \mu NLD/W/\psi^2$ is the common Sommerfeld reciprocal. N denotes the shaft speed in rev/s

and μ is the dynamic viscosity. L and D represent width and diameter of the bearing, respectively, and $\psi = C/(D/2)$ is the clearance ratio. The static bearing load is denoted by W. From (7) dimensionless bearing stiffness coefficients

$$\frac{C}{W}[K'_B] = 2\pi S \begin{bmatrix} \frac{4\varepsilon_o(1+\varepsilon_o^2)}{(1-\varepsilon_o^2)^3} & \frac{\pi}{2(1-\varepsilon_o^2)^{3/2}} \\ \frac{-\pi(1+2\varepsilon_o^2)}{2(1-\varepsilon_o^2)^{5/2}} & \frac{2\varepsilon_o}{(1-\varepsilon_o^2)^2} \end{bmatrix} \tag{18}$$

and damping coefficients

$$\frac{C\omega}{W}[C'_B] = 2\pi S \begin{bmatrix} \frac{\pi(1+2\varepsilon_o^2)}{(1-\varepsilon_o^2)^{5/2}} & \frac{-4\varepsilon_o}{(1-\varepsilon_o^2)^2} \\ \frac{-4\varepsilon_o}{(1-\varepsilon_o^2)^2} & \frac{\pi}{(1-\varepsilon_o^2)^{3/2}} \end{bmatrix} \tag{19}$$

of first order are obtained. Dimensionless second order coefficients are derived in (6) as follows

$$\frac{C^2}{W}\langle KK'_B\rangle = 2\pi S \left\langle \begin{bmatrix} \frac{4(1+8\varepsilon_o^2+3\varepsilon_o^4)}{(1-\varepsilon_o^2)^4} & \frac{3\pi\varepsilon_o}{2(1-\varepsilon_o^2)^{5/2}} \\ \text{symmetric} & \frac{2(1+3\varepsilon_o^2)}{(1-\varepsilon_o^2)^3} \end{bmatrix}_r \right. \left. \begin{bmatrix} \frac{-3\pi\varepsilon_o(3+2\varepsilon_o^2)}{2(1-\varepsilon_o^2)^{7/2}} & \frac{2(1+3\varepsilon_o^2)}{(1-\varepsilon_o^2)^3} \\ \text{symmetric} & \frac{-3\pi\varepsilon_o}{2(1-\varepsilon_o^2)^{5/2}} \end{bmatrix}_t \right\rangle \tag{20}$$

$$\frac{C^2\omega}{W}\langle KC'_B\rangle = 2\pi S \left\langle \begin{bmatrix} \frac{3\pi\varepsilon_o(3+2\varepsilon_o^2)}{(1-\varepsilon_o^2)^{7/2}} & \frac{-4(1+3\varepsilon_o^2)}{(1-\varepsilon_o^2)^3} \\ \frac{8}{(1-\varepsilon_o^2)^2} & \frac{3\pi\varepsilon_o}{(1-\varepsilon_o^2)^{5/2}} \end{bmatrix}_r \right. \left. \begin{bmatrix} \frac{-4(1+3\varepsilon_o^2)}{(1-\varepsilon_o^2)^3} & \frac{3\pi\varepsilon_o}{(1-\varepsilon_o^2)^{5/2}} \\ \frac{3\pi\varepsilon_o}{(1-\varepsilon_o^2)^{5/2}} & \frac{-8}{(1-\varepsilon_o^2)^2} \end{bmatrix}_t \right\rangle \tag{21}$$

$$\frac{C^2\omega^2}{W}\langle CC'_B\rangle = 2\pi S \left\langle \begin{bmatrix} \frac{8(3+\varepsilon_o^2)}{(1-\varepsilon_o^2)^3} & 0 \\ 0 & 0 \end{bmatrix}_r \right. \left. \begin{bmatrix} 0 & 0 \\ 0 & 0 \end{bmatrix}_t \right\rangle \tag{22}$$

It can be seen that from the twenty independent second order coefficients five are identical zero for the short journal bearing. Note that the above matrices, as indicated by a prime, correspond to a local r-t-z reference frame of the bearing. For any other x-y-z reference frame the corresponding first order coefficients are obtained from

$$[K \text{ or } C] = [T][K' \text{ or } C'][T]^T \tag{23}$$

where

$$[T] = \begin{bmatrix} \cos\Phi & -\sin\Phi \\ \sin\Phi & \cos\Phi \end{bmatrix} \tag{24}$$

is an orthogonal unitary transformation matrix with Φ being the attitude angle of the r-axis with respect to the x-axis, see Fig 1. Second order bearing coefficients corresponding to a x-y-z reference frame can be determined from

$$\langle KK\rangle = \left\langle \begin{matrix} [KK]_x \\ [KK]_y \end{matrix} \right\rangle = \left\langle \begin{matrix} [T][[KK']_r\cos\Phi - [KK']_t\sin\Phi][T]^T \\ [T][[KK']_r\sin\Phi + [KK']_t\cos\Phi][T]^T \end{matrix} \right\rangle \tag{25}$$

In Fig 2, for example, a logarithmic plot of three dimensionless second order stiffness coefficients (KK_{yxx}, $KK_{yxy} = KK_{yyx}$, KK_{yyy})C^2/W for the short journal bearing is shown in terms of the modified Sommerfeld reciprocal S as defined by Equ.(17). In this example Φ is chosen to be the load attitude angle, i.e., the x-axis is parallel with the direction of the static load.

2.4 Unbalance and shaft bow response

Both unbalance and shaft bow generate synchronous harmonic excitation forces acting upon the rotor. When introducing complex notation the right hand side of Equ.(10) can be written in the form

$$[K_S]\{\delta(t)\}+\omega^2\{U(t)\} = \{X\}\cos\omega t+\{Y\}\sin\omega t = \{R_1\}e^{i\omega t}+\{R_1^*\}e^{-i\omega t} \tag{26}$$

where $\{R_1\} = \{X-iY\}/2$ represents a complex valued first order excitation vector with $\{R_1^*\}$ being the complex conjugate of $\{R_1\}$. The components of $\{X\}$, $\{Y\}$, and $\{R_1\}$, respectively, can be obtained by inserting Equ.(1) and (5) into Equ.(26). From the linear differential operator in Equ.(10) a frequency response matrix

$$[G(i\Omega)] = [K] + i\Omega[C] - \Omega^2[M] \tag{27}$$

is defined with which a complex amplitude response vector

$$\{Z_\nu\} = [G(i\nu\omega)]^{-1}\{R_\nu\} \tag{28}$$

can be evaluated for the first order $\nu = 1$ by applying a proper solving routine for linear algebraic equations with complex coefficients. From $\{Z_1\}$ and the right hand side of Equ.(11) second order excitation vectors

$$\{R_o\} = -\frac{1}{2}\left\{\{Z_1\}^T\left\langle\left\langle KK_B\right\rangle - 2i\omega\left\langle KC_B\right\rangle + \omega^2\left\langle CC_B\right\rangle\right\rangle\{Z_1^*\}\right\} \tag{29}$$

and

$$\{R_2\} = -\frac{1}{2}\left\{\{Z_1\}^T\left\langle\left\langle KK_B\right\rangle + 2i\omega\left\langle KC_B\right\rangle - \omega^2\left\langle CC_B\right\rangle\right\rangle\{Z_1\}\right\} \tag{30}$$

are determined. A second order response $\{Z_o\}$ and $\{Z_2\}$ is then calculated from Equ.(28) for $\nu = 0$ and $\nu = 2$, respectively. According to Equ.(13) an approximate solution for the complete response of the rotor up to the second harmonic is finally obtained in the form

$$\{z(t)\} \doteq \{z_o\} + 2\mathrm{Re}\{\{Z_o\} + \{Z_1\}e^{i\omega t} + \{Z_2\}e^{i2\omega t}\} \tag{31}$$

where Re stands for real part. The static position (zero-state) of the rotor without shaft bow and unbalance is represented by $\{z_o\}$. The unbalance and shaft bow response is described by a synchronous component $\{Z_1\}$, a constant shift $\{Z_o\}$ and a nonsynchronous (twice speed) component $\{Z_2\}$. Both $\{Z_o\}$ and $\{Z_2\}$ are caused by nonlinear bearing effects. Note that $\{Z_o\}$, $\{Z_1\}$, and $\{Z_2\}$ are complex valued vectors carrying both amplitude and phase informations of the rotor response.

3 NUMERICAL RESULTS

3.1 Static bearing loads and stability thresholds

Fig 3 shows a schematic diagram of a five-stations model for a symmetric rotor. The model has two major mass stations and three bearing stations. The continuous mass of the shaft is symmetrically lumped at the five stations. In the following a vertical misalignment $m_x \neq 0$ is applied to the center bearing with respect to the outer bearings while the horizontal misalignment m_y is kept zero. Table 1 shows the rotor bearing data as used in the numerical calculation.

Table 1 Rotor and bearing data

Mass of the rotor	$2M+M_S = 16.8$ kg
Shaft stiffness	$EI = 3350$ Nm^2
Bearing span	$L = 0.24$ m

	center/outer station
Bearing length	15/7.5 mm
Journal diameter	25/12.5 mm
Clearance ratio	0.002/0.0024

In Fig 4 the dimensionless static bearing-load to rotor-weight ratio is drawn as a function of the vertical misalignment for various values of the shaft speed. The solution was obtained by applying a Newton-Raphson iteration to the nonlinear system Equ.(9). The static bearing forces $\{F_B\}$ were evaluated from the theory of short journal bearings (7). The dotted lines in Fig 4 represent asymptotic solutions corresponding to zero speed (stationary rotor) and infinite speed, respectively. Stability thresholds, limiting the speed of the real machine, are not plotted in this figure. For small positive values of vertical misalignment the center bearing load decreases slightly and approaches a minimum while the outer bearing loads increase, and vice versa for small negative misalignments. If the magnitude of misalignment becomes unrealistic high then all bearing loads increase rapidly, approaching an asymptote of which the corresponding rate of change is determined from the bending stiffness of the shaft and the bearing spans only.

In Fig 5 the load ratio for the center bearing is represented in terms of the shaft speed. Corresponding to a given vertical misalignment the zero speed load may be either zero or finite. When the speed goes to infinity the load ratio approaches an asymptotic value which is given from the dotted line ($N = \infty$) in Fig 4. For any misalignment a corresponding stability limit for the shaft speed exists which is indicated in the diagram. It is interesting to note that, in this example, small changes of the vertical misalignment do significantly influence the bearing loads while the stability threshold keeps almost unchanged.

In Fig 6(a) the stability threshold of the present rotor bearing system is shown in terms of the vertical misalignments m_x. A horizontal misalignment m_y is not applied in this example. The absolute minimum of the stability threshold of the rotor is 292 Hz and appears at a misalignment value of $m_x = -2$ µm which is about 1/10 of the center bearing clearance or 1/120000 of the outer bearing span. It can be seen that for small misalignments from -4 µm to 11 µm the stability threshold is less sensitive due to changes in the misalignment. Outside of that range the speed limit increases rapidly with increasing magnitudes of the misalignment.

A more flexible rotor is obtained by increasing the bearing span to L = 800 mm and decreasing the shaft bending stiffness to EI = 1620 Nm^2; see Table 1. The corresponding stability map is shown in Fig 6(b). Note that the stability level at zero misalignment drops down from 293 Hz for the rigid shaft to 110 Hz for the flexible one. Beside that two narrow gaps appear in the neighborhoods of $m_x = -400$ µm and $m_x = +800$ µm where the stability limit drops down dramatically within a very small range of misalignments. For example, if the center bearing of the flexible shaft version is vertically misaligned by about -1/2000 of the outer bearing span the stability threshold drops down to about 50% of the predicted value for a perfectly aligned configuration. The physical reason for the stability drop of the whole system is a substantial decrease in one of the bearing loads due to misalignment, combined with a high flexibility of the shaft. In such cases a high sensitivity of the stability limits due to changes in bearing misalignments can oc-

cur and may explain deviations between experimental results and theoretical predictions.

3.2 Nonlinear unbalance orbits

The accuracy of the perturbation approach as presented in Equ.(31) was tested by a simple inflexible Jeffcott rotor supported by two short journal bearings. The exact steady state unbalance response was obtained by numerical integration of the equations of motion. Fig 7 shows a comparison of various rotor orbits corresponding to various unbalance eccentricities. As long as the assumptions, as made in the perturbation approach, are fulfilled a very good agreement between the exact solution and the second order approximation is obtained. If the unbalance response amplitudes reach the same order of magnitude as the bearing clearance the second order approach may still be acceptable good (for example, see orbit for e = 300 μm). However, when the shaft whirls arround the bearing center the approximation is not valid any longer. Therefore, self-excited vibrations beyond the stability thresholds and unbalance response for vertical machines with cylindrical journal bearings cannot be treated by this method.

Fig 8 shows a symmetric unbalance response of a two-mass three-bearing rotor as described in Table 1. The bearings are assumed to be perfectly aligned. Note that the shaft orbits at the outer bearing stations show more nonlinear effects than the center bearing orbits. The reason is that the center bearing is less loaded and operates at a lower bearing eccentricity ratio. It may be of interest to note that once the unbalance and/or shaft bow response of first and second order is evaluated by Equ.(31) it is convenient to go back to Equ.(8) and calculate dynamic bearing loads of first and second order which may be useful for further bearing design.

4 CONCLUSION

The equations of motion for a multi-mass rotor that may be initially warped and is supported by a misaligned multi-bearing system with nonlinear characteristics are presented in this paper. The influence of bearing misalignments upon static bearing loads and stability thresholds of the rotor is investigated. It is shown that regions of extremely high sensitivity of the rotor stability limits with respect to misalignments may occur in a system. Therefore, when calculating stability maps of a rotor bearing system it is highly recommended to study the influences of bearing misalignments at the same time.

By employing the theory of short journal bearings simple analytical expressions for second order bearing coefficients are presented which make it possible to evaluate nonlinear unbalance and shaft bow response of a multi-mass multi-bearing rotor. The major advantage of the method is that once the equilibrium state of the rotor is obtained, the unbalance response up to the second harmonic is evaluated by a purely linear recursive routine. A disadvantage is that vertical rotors in cylindrical journal bearings cannot be treated. For horizontal machines the method yields good results for most of the practical applications.

REFERENCES

(1) NICHOLAS, J.C., GUNTER, E.J., ALLAIRE, P.E. Effect of residual shaft bow on unbalance response and balancing of a single flexible rotor. Part I: Unbalance response. Journal of Engineering for Power, 1976, 98, 171-181.

(2) BANNISTER, R.J.A theoretical and experimental investigation illustrating the influence of nonlinearity and misalignment on the eight oil-film force coefficients. Institute of Mechanical Engineering Conference Publications, London, 1976, C219, 271-278.

(3) GASCH, R. Berechnung der Lagerlasten mehrfach gleitgelagerter Rotoren unter Berücksichtigung des nichtlinearen Verhaltens des Ölfilms. Konstruktion, 1970, 22, 229-235.

(4) NASUDA, T., HORI, Y. Influence of misalignment of support journal bearings on stability of multi-rotor systems. Proc.IFToMM-Conf. on Rotor Dynamic Problems in Power Plants, Rome, 1982, 389-395.

(5) LUND, J.W., NIELSEN, H.B. Instability thresholds of an unbalanced, rigid rotor in short journal bearings. Inst.f.Mech.Eng.Conf. Publ., London, 1980, C263, 91-95.

(6) SPRINGER, H., GUNTER, E.J., HUMPHRIS, R.R. Nonlinear unbalance response of a multi-mass rotor-bearing system with initial shaft bow and bearing misalignment. Report, University of Virginia, ROMAC-Lab. (to appear).

(7) SZERI, A.Z. (Ed.) Tribology: Friction,lubrication and wear. Hemisphere Publ.Corp., Washington, 1980.

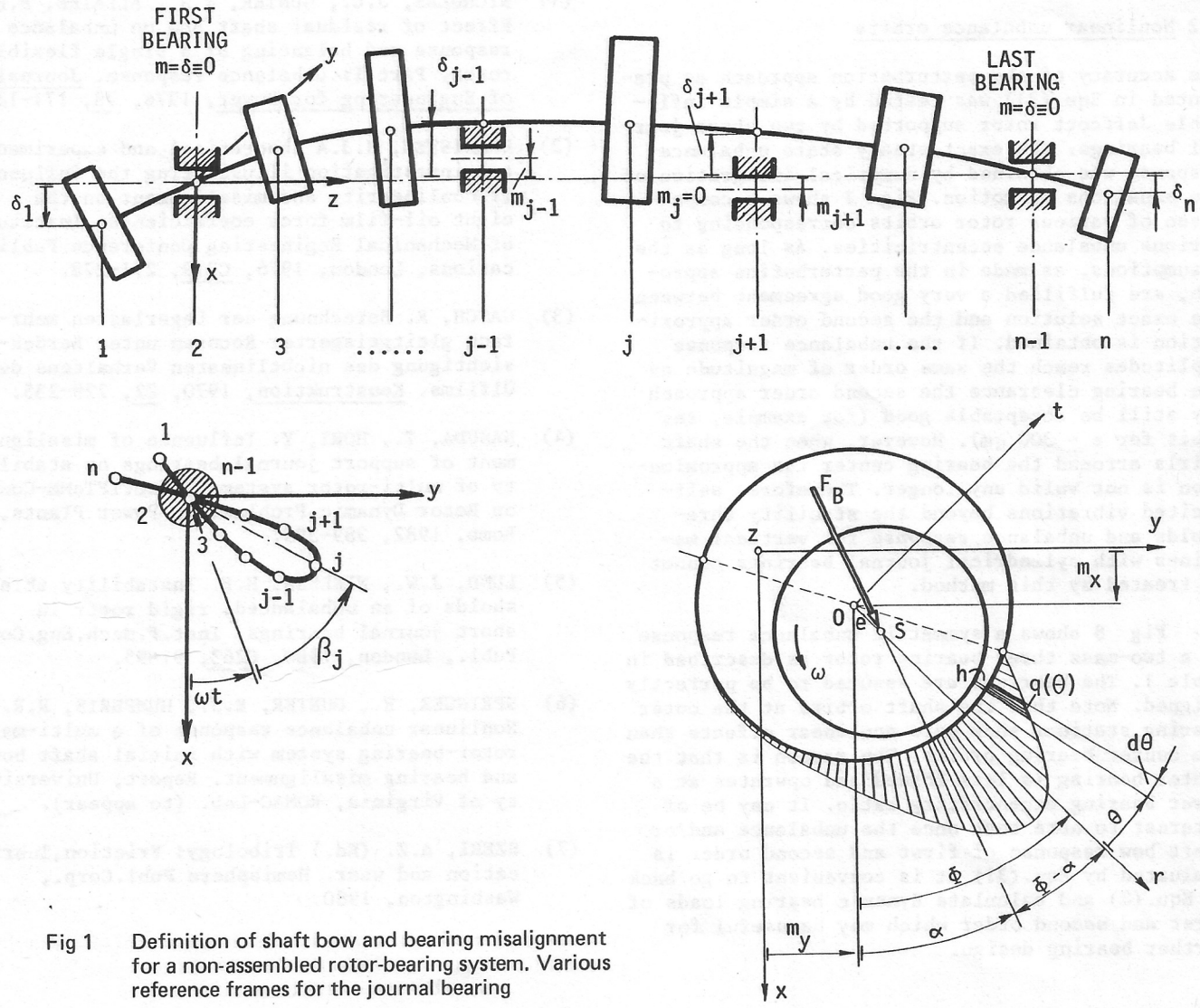

Fig 1 Definition of shaft bow and bearing misalignment for a non-assembled rotor-bearing system. Various reference frames for the journal bearing

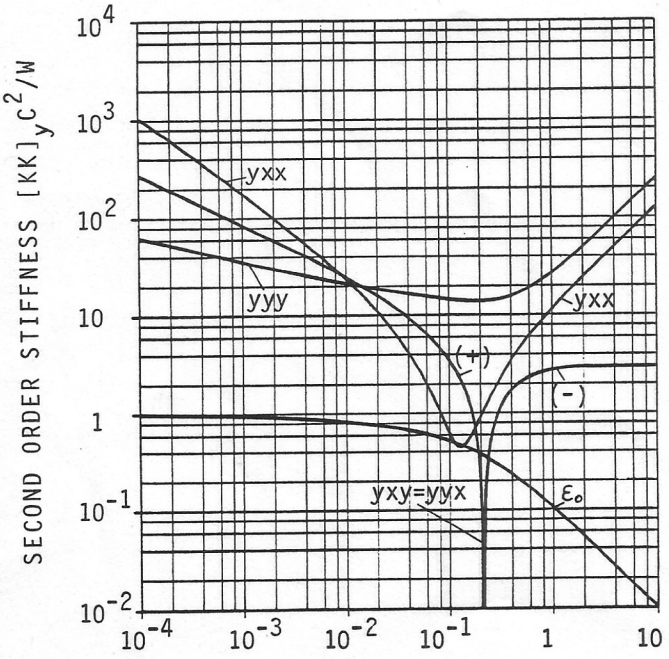

$$S = \frac{\mu NLD}{W}\left(\frac{L}{D}\right)^2$$

Fig 2 Dimensionless second order stiffness coefficients $(KK_{yxx}, KK_{yxy}=KK_{yyx}, KK_{yyy})C^2/W$ for the short journal bearing in terms of the modified Sommerfeld

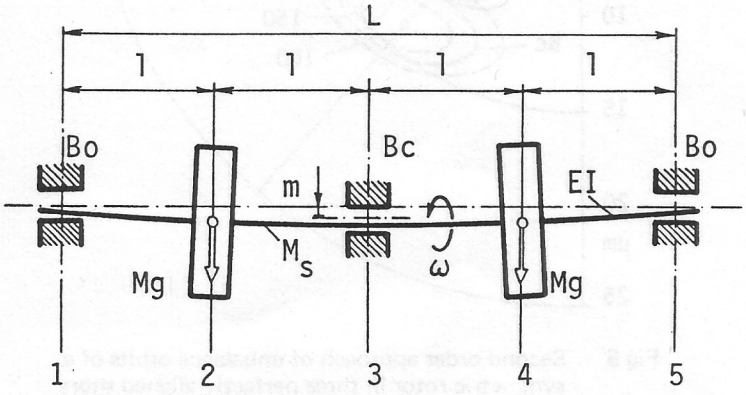

Fig 3 Five-stations model of a symmetric rotor in three misaligned journal bearings. Rotor-bearing data, see Table 1

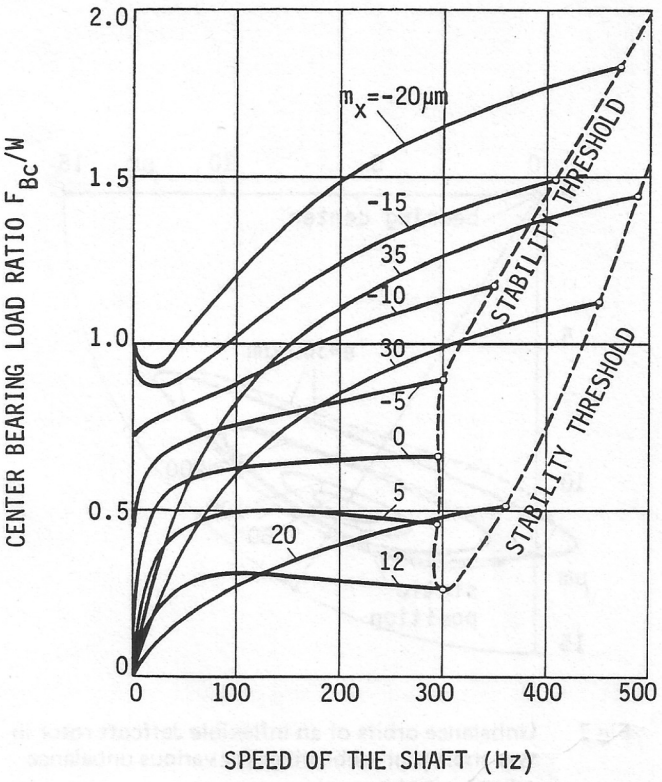

Fig 5 Dimensionless static load ratio of the centre bearing in terms of the shaft speed N for various vertical misalignments m_x. Rotor weight W=164.8 N. Rotor-bearing data, see Table 1

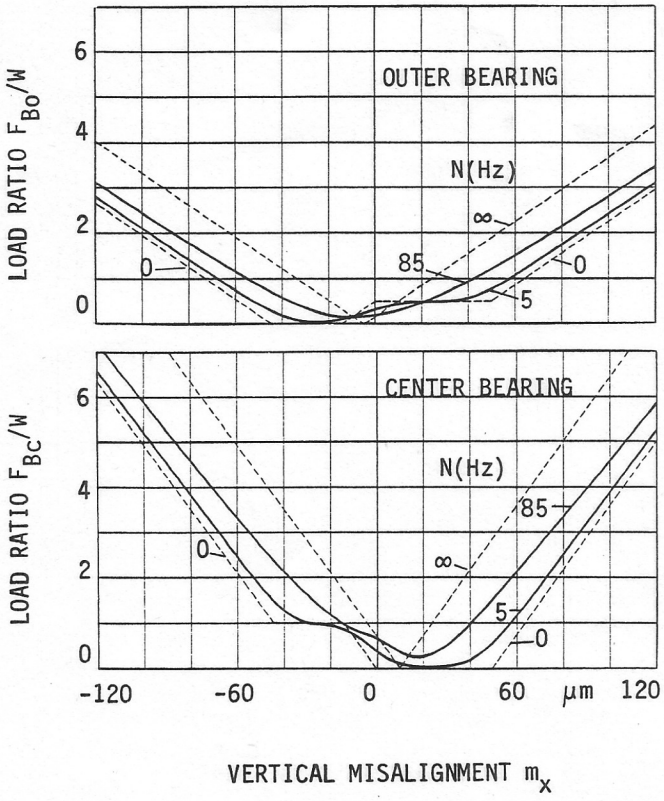

Fig 4 Dimensionless static bearing load ratios in terms of the vertical misalignment m_x for various values of the shaft speed N. Rotor weight W = 164.8 N. Rotor bearing data, see Table 1

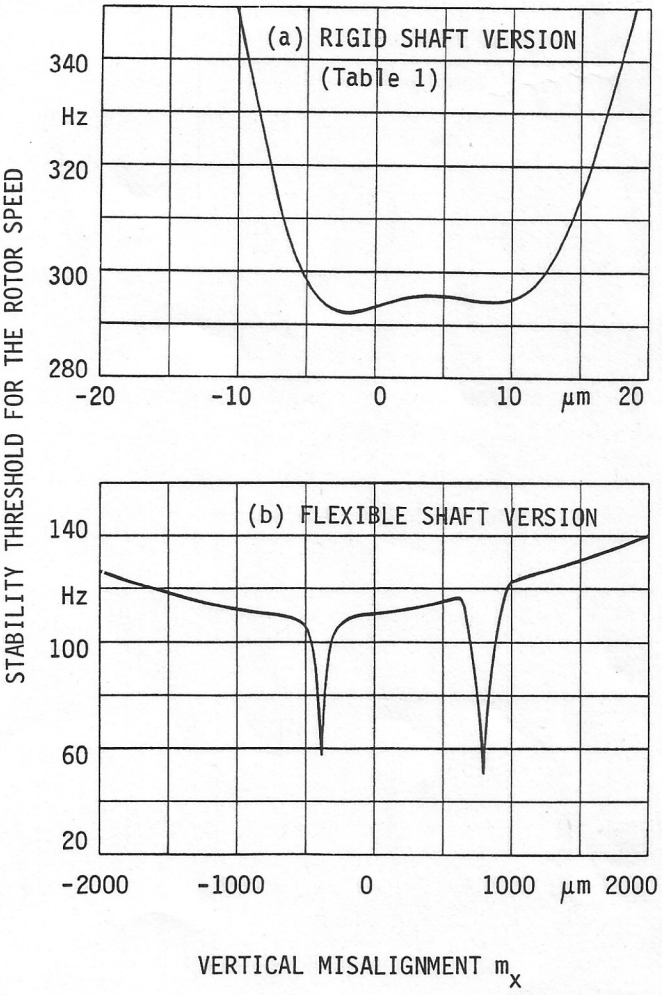

Fig 6 Stability thresholds of a symmetric rotor in three short journal bearings in terms of the vertical misalignment

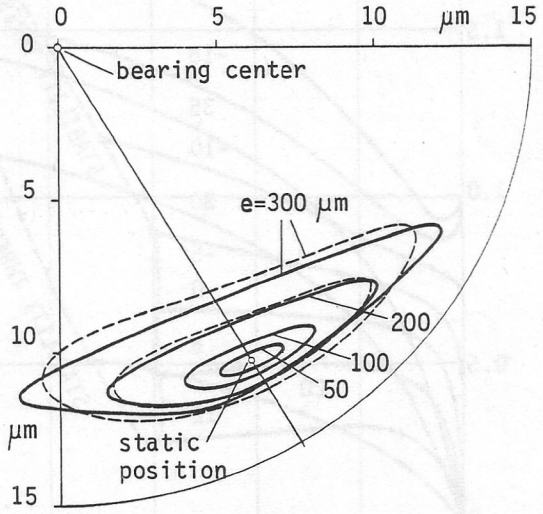

Fig 7 Unbalance orbits of an inflexible Jeffcott rotor in two short journal bearings for various unbalance eccentricities e.
——— second order perturbation approach
– – – – exact solution

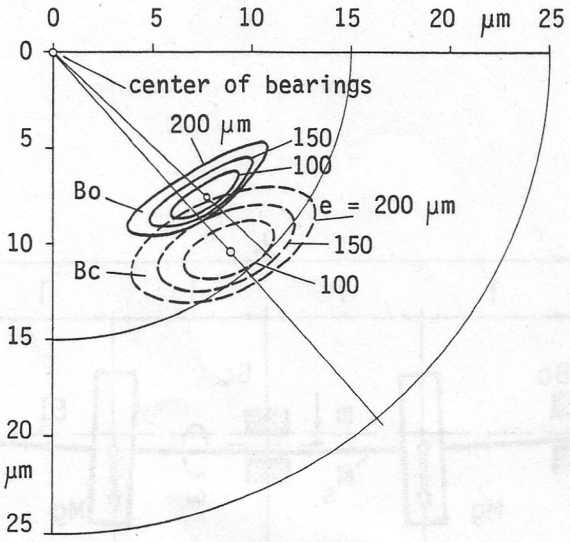

Fig 8 Second order approach of unbalance orbits of a symmetric rotor in three perfectly aligned short journal bearings for various unbalance eccentricities e. Rotor bearing data, see Table 1
——— outer bearing orbits
– – – – centre bearing orbits